OPTIMIZING DEPLOYMENT OF SPONGE ZONE ON NUMERICAL WAVE CHANNEL

Chung-Ren Chou John-Z Yim
Department of Harbor and River Engineering
National Taiwan Ocean University,
Keelung, Taiwan 202, R.O.C.

Ruey-Syan Shih*
Department of Civil Engineering
Tung Nan Institute of Technology
Taipei, Taiwan 222, R.O.C.

Key Word: boundary element, absorbing boundary, sponge zone, attenuation rate.

ABSTRACT

In this study, we used the boundary element method to simulate a two-dimensional wave tank with an absorbing boundary. The absorbing boundary, which consists of a sponge zone, is further divided into an area with a smoothly varied absorption coefficient μ and an area of constant μ. Both solitary, as well as periodic, waves are used in this study. Time histories of surface elevations are measured by a pseudo wave gage. The optimal combination of the absorption coefficient and sponge length to minimize wave reflection is investigated by studying these time series. The efficiency of the absorption zone is demonstrated by the attenuation rate of the wave energy, which for cases can reach a value of 100%. Based upon the present results, it is recommended that in simulating solitary waves, a value of μ_0=0.5 for the absorption coefficient with a sponge length of 15~25 times the water depth is ideal; whereas a value of μ_0=1.0 in combination with a sponge length 20 times the water depth should be used for periodic waves.

I. INTRODUCTION

Recently, the adoption of dissipating terms in the form of absorbing beaches and/or sponges has become an interesting technique for simulations in numerical wave tanks. As a result of the progress in computer technology nowadays, numerical wave models have been largely developed. To decrease the influences of reflected waves, wave absorption zones have been widely used in these numerical models. Either these absorption zones are assumed to be of infinite length, or it is assumed that wave energies are completely absorbed.

It is well known, however, that a numerical model should have a limited domain. To circumvent this difficulty, many researches resort to the fact that wave reflections can be reduced by imposing an open boundary behind the domain. The concept of "absorbing beach" was first proposed by Le Méhauté in 1972. In their numerical scheme for random wave simulations, Larsen and Dancy (1987); Brorsen and Larsen (1987) adopted this idea successfully.

*Correspondence addressee

Ohyama and Nadaoka (1991) modelled the evolution of nonlinear and irregular waves in a numerical wave tank. For open boundary condition, a numerical wave absorption filter was used in their analysis. This filter is composed of a simulated sponge layer and Sommerfeld's radiation condition at the outer edge of the layer. This method has been used previously by Ijima et al. (1971) and Chou (1976) in their investigations of permeable coastal structures.

The absorbtion of free surface waves including periodic boundary condition, matching to a simplified outer solution, radiation conditions and absorbing beach are discussed by Gao *et al.* (1993), the efficiencies of various types of absorbing beaches with pressure terms of $P=\nu\phi$ and $P=\nu\phi_n$ are compared, where ν is the damping term and ϕ_n denotes the normal derivative of the potential energy ϕ on the free surface. Based on Sommerfeld's condition, Grilli *et al.* (1995, 1997) developed an implicit iterative radiation condition as boundary condition. The numerical scheme was used successfully in the calculations of the shoaling and breaking of both periodic and solitary waves over gentle slopes. Dalrymple *et al.* (2000) studied the characteristics of the wave fields around an idealized inlet of a bay. Depending on whether the inlet sidewalls are reflective or absorbent, two different mathematical treatments were used.

In this article, the case of a numerical wave flume with a closed boundary condition at one end was considered. At this end, a sponge zone was imposed. The sponge zone is composed of two regimes with different absorption coefficients μ, i.e., a zone with smoothly varied μ and a zone with constant μ. The main purpose of this article is to determine the optimum combination of the value of the absorption coefficient and the length of the sponge zone through which wave reflections can be minimized.

II. NUMERICAL MODELING

The deformation and absorption of solitary and regular waves are simulated by means of boundary element method. As shown in Fig.1, the numerical wave channel is confined in a region composed of: a moving wave-making paddle, the undisturbed free water surface, an impermeable seawall and the impermeable seabed. The flow within the region was assumed to be inviscid, incompressible and irrotational.

Boundaries in the regime of the numerical analyses are discretized using linear elements. The continuity equation is solved using the linear boundary element method based on the Green's second identity, where the velocity potential satisfies the following Laplace equation:

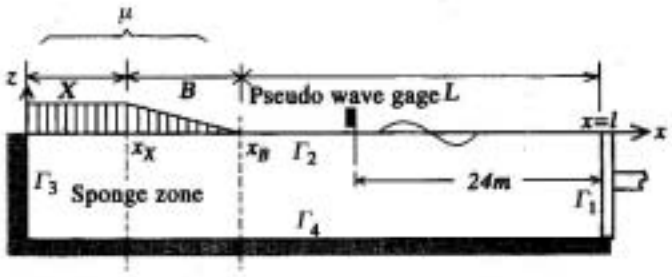

Fig. 1 Definition sketch of an absorbing wave channel

$$\frac{\partial^2\Phi}{\partial x^2}+\frac{\partial^2\Phi}{\partial z^2}=0 \tag{1}$$

1. Boundary Conditions

(i) Free Water Surface

Boundary conditions on the undisturbed free water surface can be obtained from the nonlinear kinematic and dynamic conditions and are expressed as:

$$u=\frac{Dx}{Dt}=\frac{\partial\Phi}{\partial x} \tag{2}$$

$$w=\frac{Dz}{Dt}=\frac{\partial\Phi}{\partial z} \tag{3}$$

$$\frac{D\Phi}{Dt}+g\zeta-\frac{1}{2}[(\frac{\partial\Phi}{\partial x})^2+(\frac{\partial\Phi}{\partial z})^2]+\frac{P}{\rho}=0 \tag{4}$$

with D is the Lagrange differentiation, g the gravitational acceleration, ζ the surface elevation, ρ, the fluid density and P is the atmospheric pressure. On the non-absorbing area, the atmospheric pressure is assumed to be constant, e.g., $P=0$.

On the left side of the flume, hereafter referred to as the sponge zone, an imaginary pressure term was imposed on the water surface which brought about a negative work against incident waves. According to the suggestions of Cao *et al.* (1993), the value of this pressure term, P, was defined proportional to the normal derivative of the potential energy on the free surface, and is employed by Grilli (1995) as:

$$P(x,\zeta)=\mu(x)\frac{\partial\Phi}{\partial n}(\zeta(x)) \tag{5}$$

$$\mu(x)=\mu_0\rho\sqrt{gh}(\frac{x-x_l}{l})^\alpha \tag{6}$$

where μ_0 is a non-dimensional absorption coefficient which varies as a function of space, x_l is the position measured away from the left side end where the sponge zone begins. The length of the sponge zone is denoted as l, and finally, the exponent value of the exponent α usually has values in the range of α=2–3.

In the present research, however, the value of P

was defined proportional to the free surface potential as in most of the earlier approaches suggested, thus, $P(x,\zeta)$ is expressed through:

$$P(x,\zeta)=\mu(x)\Phi(\xi,\eta,t) \tag{7}$$

$$\mu(x)=\mu_0\rho(\frac{x_B-x}{B})^{\alpha},\ x_X<x<x_B \tag{8}$$

$$\mu(x)=\mu_0\rho,\ x\le x_X \tag{9}$$

where x_X and x_B are the horizontal coordinates of the beginning of the constant μ regime and smoothly varied μ regime with the lengths of B and X, respectively. A linear absorption parameter is adopted in this paper, i.e. α=1 (as shown in Fig.1).

The physical meaning of the absorbing area (referred to as the sponge zone) can be a representative of various kinds of armor units placed behind the wave flume which exert a damping coefficient. Generally, the damping coefficient was assumed to remain constant and proportioned with potential energy or velocity of fluids. This procedure caused the region to form into two domains (considering the continuity of the potential energy and its normal derivative). As was mentioned, the numerical scheme was established using BEM. Two-dimensional problems are solved by integration over a line. The simulation of the fully nonlinear water wave in the time domain became very complicated under this circumstance. The smoothly varied μ area used here is to connect the constant μ area and the non-absorbing area as a result of the continuation of the velocity potential between these two areas, as shown in the definition sketch, the velocity potential and its normal derivative on both sides of the pseudo boundaries (dotted lines) are equivalent, therefore the flume can be considered as one domain and make the calculation easier.

(ii) Impermeable Seawall and Seabed

The water particle velocity is null in the normal direction on the impermeable seawall and seabed, therefore the condition is prescribed as

$$\frac{\partial\Phi}{\partial n}=0 \quad \text{on } \Gamma_3 \text{ and } \Gamma_4 \tag{10}$$

where n is the unit outward normal vector.

(iii) Pseudo Wave Paddle

A piston type wavemaker is adopted in this study to simulate the process of wave generation. The associated boundary condition is obtained by matching the horizontal velocities of the wave-paddle and that of the fluid flow through:

$$\bar{\Phi}=\frac{\partial\Phi}{\partial n}=-U(t) \tag{11}$$

For a solitary wave, according to the Boussinesq equation, $U(t)$ can therefore be expressed as:

$$U(t)=\zeta_0\sqrt{\frac{g}{h}}\cdot\sec h^2[\sqrt{\frac{3\zeta_0}{4h^3}}C(t-t_c)] \tag{12}$$

where ζ_0, h, C and t_c are the incident wave height, water depth, wave celerity and specific time of the semistroke of the paddle, respectively.

For periodic waves, $U(t)$ is expressed as:

$$U(t)=\zeta_0\frac{\sinh kh\cosh kh+kh}{2\sinh^2 kh}\sigma\sin\sigma t \tag{13}$$

where σ (=$2\pi/T$), k and T are the angular frequency, the wave number and wave period individually.

2. Governing Equations and boundary discretization

The governing equations and numerical methods are briefly reviewed in the following, details can be found in Chou and Shih (1996). According to Green's second identity, the velocity potential $\Phi(x,z;t)$ for inviscid irrotational flow can be obtained by the velocity potential on the boundary, $\Phi(\xi,\eta;t)$, and its normal derivative, $\partial\Phi(\xi,\eta;t)$, thus,

$$c\Phi(x,z;t)=\frac{1}{2\pi}\int_\Gamma[\frac{\partial\Phi(\xi,\eta;t)}{\partial n}\ln\frac{1}{r}-\Phi(\xi,\eta;t)\frac{\partial}{\partial n}\ln\frac{1}{r}]ds \tag{14}$$

$$c=\begin{cases}1 & \text{inside the fluid domain}\\ 1/2 & \text{on the smooth boundary}\\ 0 & \text{outside the fluid domain}\end{cases}$$

with $r=[(\xi-x)^2+(\eta-z)^2]^{1/2}$

As shown in Fig. 1, the boundaries Γ_1 through Γ_4 are devided into N_1 to N_4 discrete segments with linear elements in order to proceed with the calculations. When the inner point $(x,z;t)$ approaches the boundary point $(\xi',\eta';t)$, Eq. (14) can be written in a discretized form as.

$$\Phi_i(\xi',\eta';t)+\frac{1}{\pi}\sum_{j=1}^{N}\int_{\Gamma_j}[\Phi_j(\xi,\eta;t)M_1+\Phi_{j+1}(\xi,\eta;t)M_2]\frac{\partial}{\partial n}\ln\frac{1}{r}ds$$

$$=\frac{1}{\pi}\sum_{j=1}^{N}\int_{\Gamma_j}[\frac{\partial\Phi_j}{\partial n}(\xi,\eta;t)M_1+\frac{\partial\Phi_{j+1}}{\partial n}(\xi,\eta;t)M_2]\ln\frac{1}{r}ds \tag{15}$$

with $M_1=(1-\chi)/2$, $M_2=(1+\chi)/2$; M_1 and M_2 are the

shape function within χ which is a local dimensional coordinate.

Hence, Eq.(15) is expressed in a matrix form:

$$[\Phi_i]=[O_{ij}][\bar{\Phi}_i] \quad i, j=1\sim4 \tag{16}$$

where $[\Phi]$ and $[\bar{\Phi}]$ are the nodal values of the potential function and its normal derivative on the boundaries, respectively, and $[O]$ is a matrix related to the geometrical shape of the boundary. The numerical scheme has been discussed in detail by Chou (1976).

3. Computational Procedure

The initial conditions are summarized as follows: Requiring that the horizontal velocity of the pseudo wave paddle $U(t)$ and the fluid motion be continuous, we obtain $\Phi_1^0=\partial\Phi_1^0/\partial n=-U(0)$. Assume that the water surface is initially at rest, which leads to the condition that the velocity potential $\Phi_2^0=0$. Along the impermeable seawall and the stationary bottom, no flow exists in the normal direction, so that $\bar{\Phi}_3^0=\partial\Phi_3^0/\partial n=0$. In the following, the superscripts are used to denote time steps, and the subscripts are used for the respective boundaries.

To start with, the initial values for the four unknowns, i.e., the normal derivative of the velocity potential on the water surface, $\partial\Phi_2^0/\partial n$; the velocity potential on the pseudo wave paddle, Φ_1^0; and the two velocity potentials on the sea wall and seabed, Φ_3^0 and Φ_4^0, can be obtained by substituting the initial boundary conditions into Eq. (16). Using Eqs. (2)~(4), the new position for each nodal point on the water surface at the k+1-th time step (k=0, 1, 2, 3....) can be calculated using the forward difference method. The velocity potential of the free water surface at the k+1-th time step Φ_2^{k+1} can then be approximated through the following equation:

$$\Phi_2^{k+1}=\Phi_2^k+\frac{1}{2}[(\frac{\partial\Phi_2}{\partial s})^2+(\frac{\partial\Phi_2}{\partial n})^2]^k\Delta t-gz^{k+1}\Delta t-\frac{P^k}{\rho}\Delta t \tag{17}$$

where s is the tangential derivative, Δt denotes the discrete time differencing interval.

By substituting Eqs. (10), (11) and (17) into Eq. (16), we obtain the following simultaneous equations:

$$\begin{bmatrix}\Phi_1\\ \bar{\Phi}_2\\ \Phi_3\\ \Phi_4\end{bmatrix}^{k+1}=\begin{bmatrix}I & -O_{12} & 0 & 0\\ 0 & -O_{22} & 0 & 0\\ 0 & -O_{32} & I & 0\\ 0 & -O_{42} & 0 & I\end{bmatrix}^{-1}\begin{bmatrix}O_{11} & 0 & O_{13} & O_{14}\\ O_{21} & -I & O_{23} & O_{24}\\ O_{31} & 0 & O_{33} & O_{34}\\ O_{41} & 0 & O_{43} & O_{44}\end{bmatrix}\begin{bmatrix}\bar{\Phi}_1\\ \Phi_2\\ \bar{\Phi}_3\\ \bar{\Phi}_4\end{bmatrix}^{k+1} \tag{18}$$

I is a unit matrix. Detailed description concerning the iterative scheme of time stepping can be found in Chou and Shih (1996).

III. RESULTS AND DISCUSSIONS

1. Variation of Surface Elevation

A 50m long wave channel with a constant depth of h=1 m is used in the numerical simulation. As mentioned earlier, a sponge zone is fixed at the left end of the flume. The sponge zone is further divided into a smoothly varied μ area and a constant μ area, the lengths of which are expressed as B and X respectively. To study the absorption of wave energy, initial wave heights of ζ_0/h=0.05, 0.1, 0.2 and 0.3 are used for solitary waves. On the other hand, a dimensionless angular frequency of σ^2h/g=0.50 and a wave height of ζ_0/h=0.05 is used for the case of periodic waves. To determine the optimum combination of the absorption coefficient and the sponge length that can minimize wave reflection, lengths of X=5, 10, and 15 m and B=5, 10, and 15 m are used in the simulation. Furthermore, values of the absorption coefficient are varied, μ_0=0~0.5 with an increment of 0.05. Throughout the calculation a time discretization of $\Delta t=t_c/200$ is used.

Surface elevations were measured by a pseudo wave gage located at a position of x=24 m. Hence, with μ_0=0.0 a reflected wave height of ζ/h=0.05 for the case with an incident wave height of ζ_0/h=0.05 will indicate that the waves are completely reflected. Altering the lengths of the sponge zone in various combinations of X and B makes it possible to determine the optimal configuration of the sponge zone.

Figure 2 shows the variations of surface elevations with the condition of ζ_0/h=0.05, B=15 m, X=10 m and μ_0=0~0.5. To facilitate comparison, both incident and reflected waves are shown in all the figures. The curves on the left part of all the figures are the elevations of initial waves, and those on the right parts show that of the reflected waves. It can be seen that all the incident waves are identical, while the reflected wave heights decrease gradually with increasing values of μ_0. In fact, the dimensionless heights of the reflected waves, ζ_r/h, for cases with μ_0=0.1, 0.2, and 0.3 are, respectively, 0.027, 0.015, and 0.008. It decreases to a value of 0.00087 for the case with μ_0=0.5, which can be considered as null for practical applications.

2. Attenuation Rate of Wave Energy

To investigate the absorption rate resulting from the combinations of various values of B, X and μ_0, we have calculated the energies of the waves. The

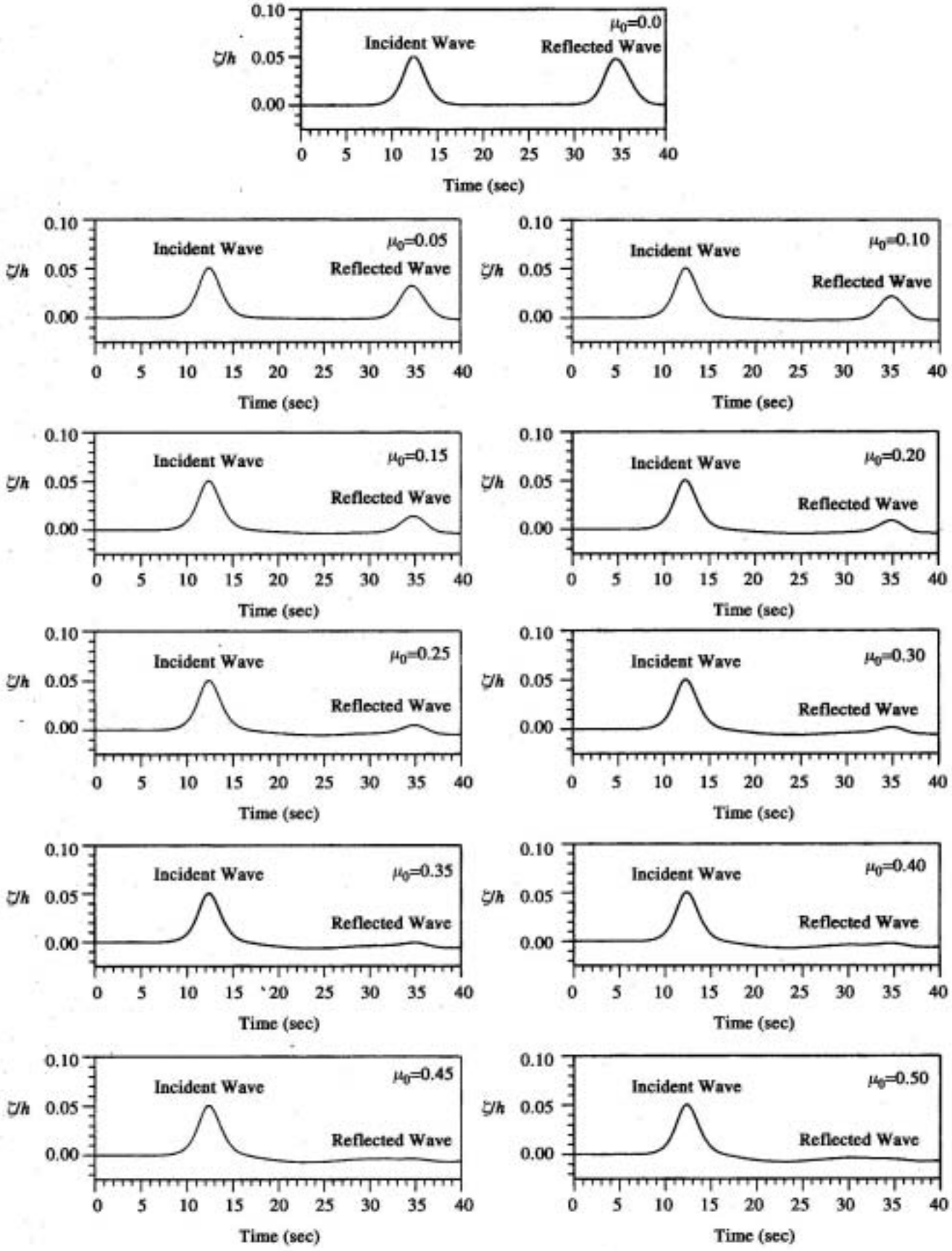

Fig. 2 Variation of surface elevations with the condition of X=15m,B=10m,ζ_0/h=0.05 and μ_0=0~0.5

total energy of a solitary wave can be expressed as:

$$E=\frac{8}{3}\rho g h\zeta\sqrt{\frac{\zeta}{3h}} \tag{19}$$

The attenuation rate can thus be calculated by:

$$K_L=(1-\frac{E_R}{E_I})\times 100\% \tag{20}$$

where K_L is the attenuation rate, E_I and E_R are the total energy of the incident and reflected wave, respectively.

Table 1. The Attenuation rate of wave energy for solitary wave
(ζ_0/h: Incident wave; ζ_r/h: Reflected Wave; K_L: Attenuation rate)

	μ_0	0.05	0.10	0.15	0.20	0.25	0.30	0.35	0.40	0.45	0.50
	ζ_0/h	0.0506	0.0506	0.0506	0.0506	0.0506	0.0506	0.0506	0.0506	0.0506	0.0506
X=15	ζ_r/h	0.0360	0.0270	0.0204	0.0154	0.0117	0.0088	0.0066	0.0049	0.0035	0.0025
B=5	K_L	39.92	61.00	74.46	83.20	88.94	92.75	95.30	97.00	98.15	98.91
	ζ_0/h	0.0517	0.0517	0.0517	0.0517	0.0517	0.0517	0.0517	0.0517	0.0517	0.0517
X=15	ζ_r/h	0.0350	0.0250	0.0179	0.0126	0.0087	0.0058	0.0035	0.0018	0.0004	0.0
B=10	K_L	44.29	66.31	79.66	87.91	93.06	96.26	98.22	99.36	99.92	100.0
	ζ_0/h	0.0505	0.0505	0.0505	0.0505	0.0505	0.0505	0.0505	0.0505	0.0505	0.0505
X=15	ζ_r/h	0.0322	0.0216	0.0141	0.0087	0.0047	0.0017	0.0	0.0	0.0	0.0
B=10	K_L	49.04	72.10	85.30	92.91	97.19	99.40	100	100	100	100
	ζ_0/h	0.0518	0.0518	0.0518	0.0518	0.0518	0.0518	0.0518	0.0518	0.0518	0.0518
X=10	ζ_r/h	0.0399	0.0322	0.0261	0.0212	0.0173	0.0141	0.0115	0.0094	0.0076	0.0062
B= 5	K_L	32.51	51.12	64.34	73.84	80.77	85.81	89.53	92.29	94.33	95.86
	ζ_0/h	0.0517	0.0517	0.0517	0.0517	0.0517	0.0517	0.0517	0.0517	0.0517	0.0517
X=10	ζ_r/h	0.0381	0.0297	0.0232	0.0182	0.0143	0.0112	0.0087	0.0068	0.0052	0.0040
B=10	K_L	36.69	56.59	70.01	79.18	85.52	89.95	93.06	95.23	96.77	97.86
	ζ_0/h	0.0517	0.0517	0.0517	0.0517	0.0517	0.0517	0.0517	0.0517	0.0517	0.0517
X=10	ζ_r/h	0.0364	0.0270	0.0202	0.0150	0.0110	0.0079	0.0055	0.0036	0.0021	0.0009
B=15	K_L	40.98	62.16	75.63	84.40	90.18	94.00	96.51	98.15	99.18	99.78
	ζ_0/h	0.0509	0.0509	0.0509	0.0508	0.0508	0.0508	0.0508	0.0508	0.0508	0.0508
X= 5	ζ_r/h	0.0424	0.0367	0.0318	0.0276	0.0241	0.0210	0.0182	0.0159	0.0139	0.0121
B= 5	K_L	24.03	38.81	50.54	59.92	67.46	73.53	78.45	82.46	85.71	88.37
	ζ_0/h	0.0518	0.0518	0.0518	0.0518	0.0518	0.0518	0.0518	0.0518	0.0518	0.0518
X= 5	ζ_r/h	0.0414	0.0345	0.0289	0.0243	0.0204	0.0172	0.0145	0.0122	0.0103	0.0086
B=10	K_L	28.67	45.70	58.35	67.95	75.25	80.87	85.21	88.56	91.17	93.20
	ζ_0/h	0.0507	0.0506	0.0506	0.0506	0.0506	0.0506	0.0506	0.0506	0.0506	0.0506
X= 5	ζ_r/h	0.0388	0.0312	0.0252	0.0204	0.0165	0.0134	0.0109	0.0088	0.0071	0.0056
B=15	K_L	33.09	51.73	64.95	74.45	81.33	86.37	90.06	92.78	94.79	96.28

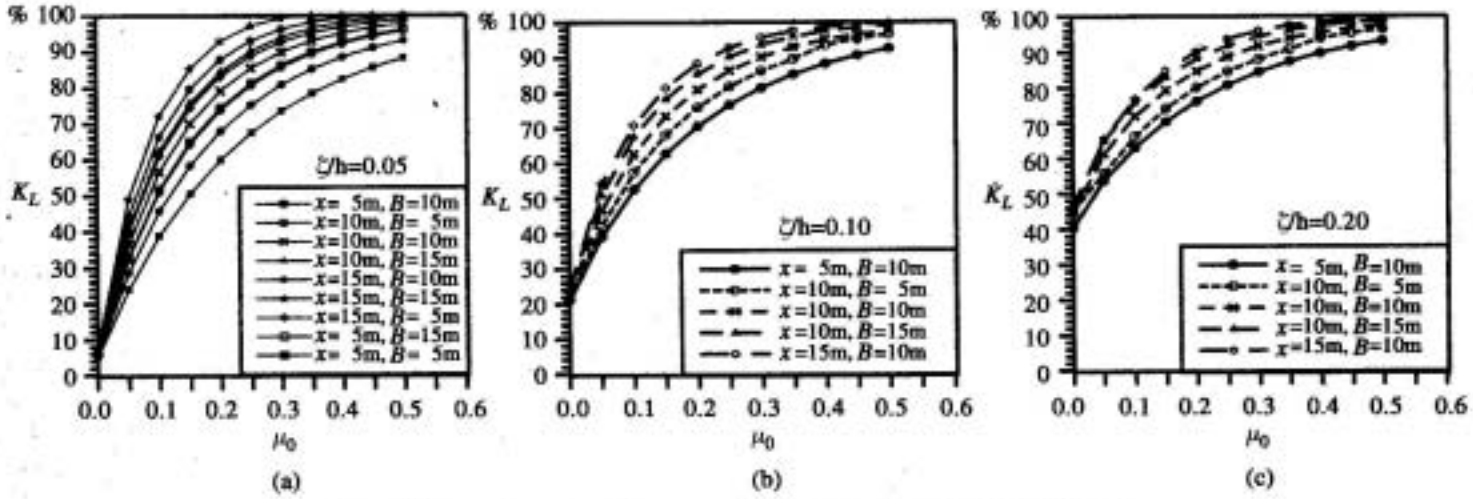

Fig. 3 Attenuation rate of the wave energy among various sponge lengths

The attenuation rates for cases of solitary waves as calculated using Eq. (20) are shown in Figs. 3(a) ~3(c). Changing the length of the smoothly varied μ area has apparently raised the absorption efficiency. Table 1 shows the reflected wave heights and attenuation rates for the cases when X is fixed with a constant value of 5 m. In the table, B=5, 10, and 15 m whereas values of μ_0 were varied from 0.05 to 0.50. Referring to Table 1 and taking Fig. 3(a) for an example, the attenuation rate of the wave energy is

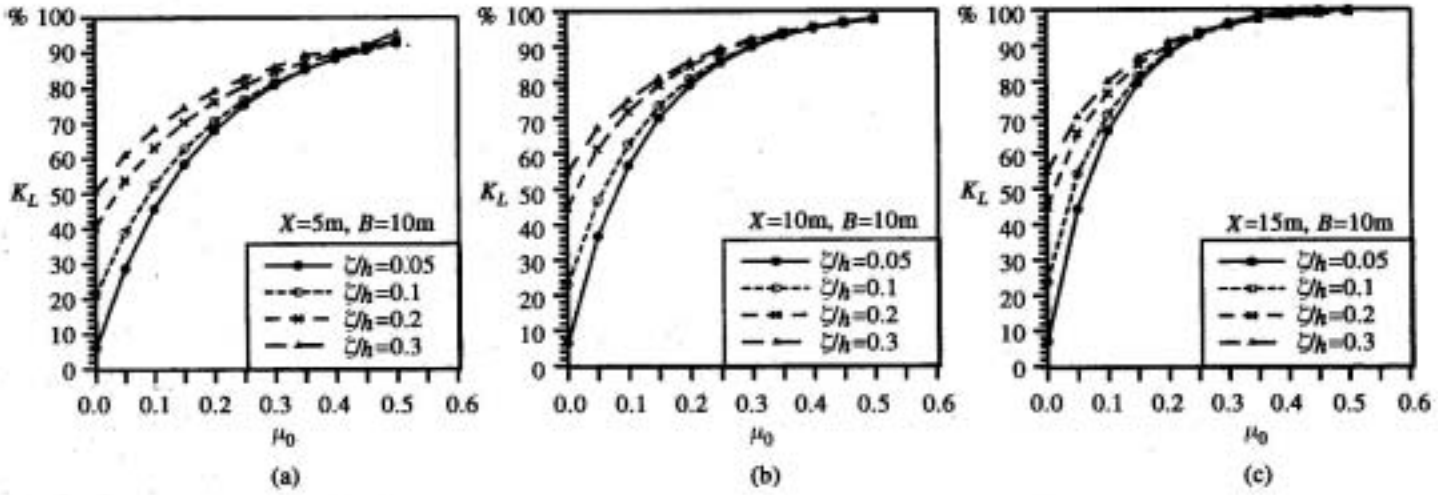

Fig. 4 Attenuation rate of the wave energy among various wave heights

93.2% for B=10 m, X=5 m and μ_0=0.5. It increases up to nearly 100% for the case with B=10 m, X=15 m and μ_0=0.5, indicating an almost complete dissipation. It can be shown that the curves grow more gently afterwards, i.e. it takes a much larger μ_0 for a further increase of the attenuation rate. This means that the effect of attenuation is limited when the absorption coefficient μ_0 has values greater than 0.5. A more effective way is to increase the length of the sponge zone, but this will require a much larger amount of nodal points and a much longer time of calculation and computer capacity. As a compromise, it is therefore decided to find an optimum combination of the present absorption coefficients and a moderate sponge length to minimize the reflection.

Figures 4(a)~4(c) show the attenuation rates for various wave heights. It can be seen from these figures that an attenuation rate of approximately 50% has already been achieved even when μ_0 only has a value of 0.1. It is also interesting to note that unfavorable results are obtained for cases with μ_0=0. The incident wave heights are seen to rise up gradually. This may be due to the insufficiency of the amount of elements on the water surface since we adopt stationary segment as Δs=1h, where Δs denotes the distance between two nodes. It can also be seen from these figures that a substantial increase of the attenuation rate can be achieved by increasing the values of the absorbing coefficient, μ_0. However, this effect is limited for values of μ_0<0.3. It is also seen that the attenuation rates approach to the same value for $\mu_0 \geq 0.3$, irrespective of the wave heights considered. This indicates that the maximum effect of the absorbing coefficient has been reached.

3. The absorption of solitary waves

Figure 5 shows time histories of the incident and reflective solitary waves. The case studied has X=15

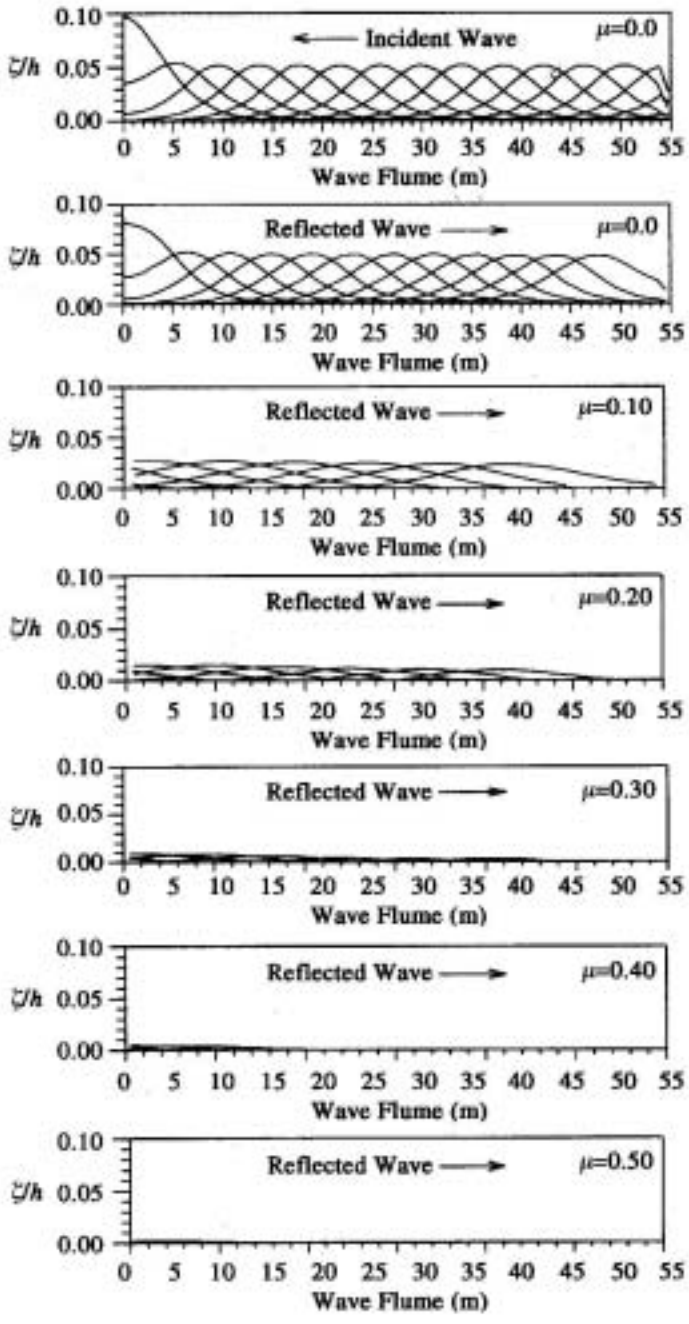

Fig. 5 Time histories of the incident and reflective waves for the case with X=15m, B=10m and ζ_0/h=0.05

m, B=10 m and ζ_0/h = 0.05. The first figure on top shows the times histories of the incident waves, while other figures show those of the reflected waves. Starting from the second figure on top to the last figure at the bottom, the values of the absorbing coefficient increase continuously.

Referring back to Table 1, it can be seen that with an absorbing coefficient of μ_0=0.5 and a constant value of X=5m, the reflected wave heights, ζ_r/h, for B=5, 10 and 15 m are 0.0121, 0.0086 and 0.0056, respectively. This clearly demonstrates that better absorbing effects can be acquired through the use of B=15m rather than B=5 m. However, it is also seen that a larger μ_0 will then be required, i.e. μ_0= 0.4~0.5. On the other hand, with the same value of μ_0=0.5 and a constant value of B=5m, the reflected wave heights ζ_r/h for X=5, 10 and 15 m are, respectively equal to 0.0121, 0.0062 and 0.0025. Furthermore, for the same total length of the sponge zone X+B, comparing the results for B=5 and X=5,10 and 15m with the cases for X=5m, while B is varied correspondingly, it can be seen from the table that the reflected wave heights are smaller for the former cases. It can also be seen from the table that for B=5m, the results are similar for X=5m with μ_0= 0.25~0.40, and for X=15m with, however, a smaller range of μ_0=0.20~0.30. The results indicate that better absorption effects can be achieved when in the sponge zone a longer X is used instead of B.

4. Absorption of Periodic Waves

To investigate the absorption of periodic waves, a 60 m long channel was used. The wave has a dimensionless angular frequency, σ^2h/g, of 0.50, and the dimensionless wave height, ζ_0/h, is 0.05. A constant water depth of h=1 m is used in the calculation. The sponge zone has a configuration similarly to that used for solitary waves. Both the constant-valued absorbing coefficient zone, X, and the gradually varied absorbing coefficient zone, B, have lengths equal to 10 m. As before, the values of the absorbing coefficient, μ_0, were varied from 0 to 1.0 with an increment of 0.2. A Δt=T/200 for the temporal, and a Δs=0.2h for the spatial, discretizations were used in all simulations.

Unlike for the cases with solitary waves where only one single crest is to be generated, the wave paddle must move back and forth continuously for periodic waves. When the waves have reached the permeable wall, clapotis will be gradually formed as a result of the intersection between incident and reflected waves. Measuring reflections for the case of periodic waves in a numerical wave tank are therefore more involved. In the present paper, we will not discuss the attenuation rate, instead, we concentrate

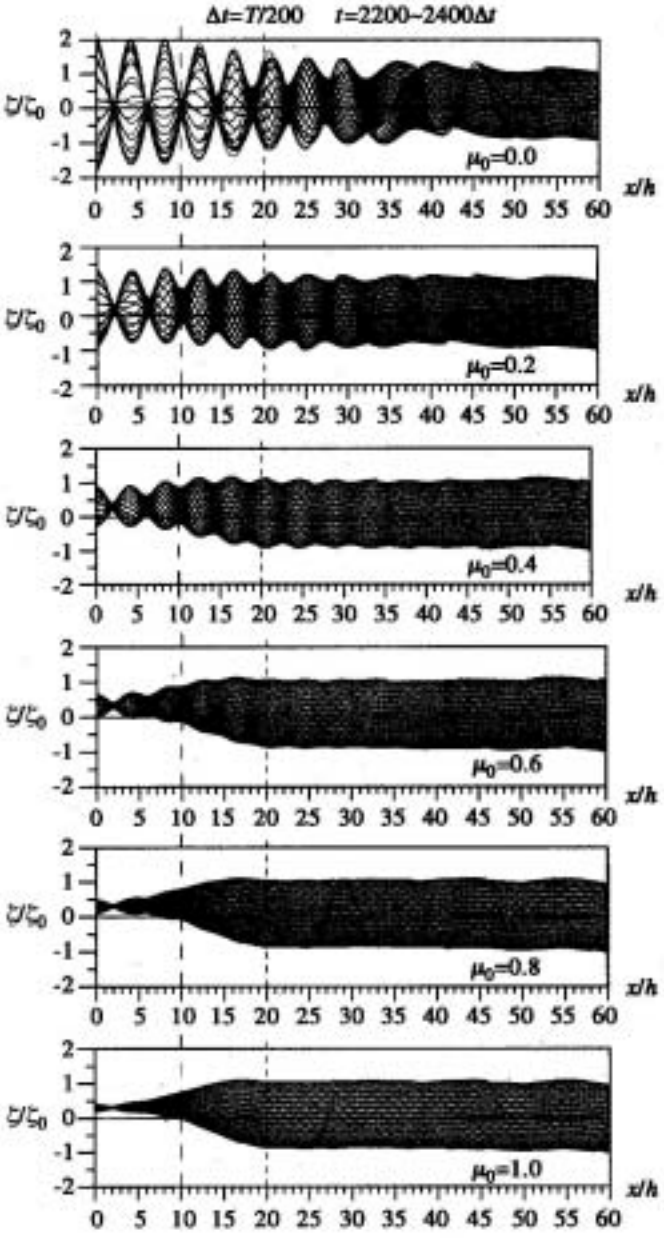

Fig. 6 Time histories of progressing and reflected periodic waves with X=10m, B=10m, σ^2h/g=0.5 and ζ_0/h=0.05 regarding different dissipation coefficient μ_0.

on the absorption, which can be determined by comparing the time histories of wave profiles.

As shown in Fig. 6, clapotis is formed completely with two times the height of the incident waves when μ_0=0. The clapotis is seen to move gradually toward the wave paddle, indicating that waves are completely reflected. Also shown in Fig. 6 are the time histories of the wave profiles for cases with absorbing coefficient μ_0 varied from 0.2 to 1.0. As can be seen from Fig. 6, when μ_0 has a value of 0.2, the height of the calpotis is about one times the incident wave height in the dimensionless distances of x/h=0~20. Compared with the envelopes of the partial standing waves in the dimensionless distances of x/h=20~60, the influence of reflected waves can be easily perceived. This phenomenon will be improved only when μ_0 has a value greater than 0.6. The waves

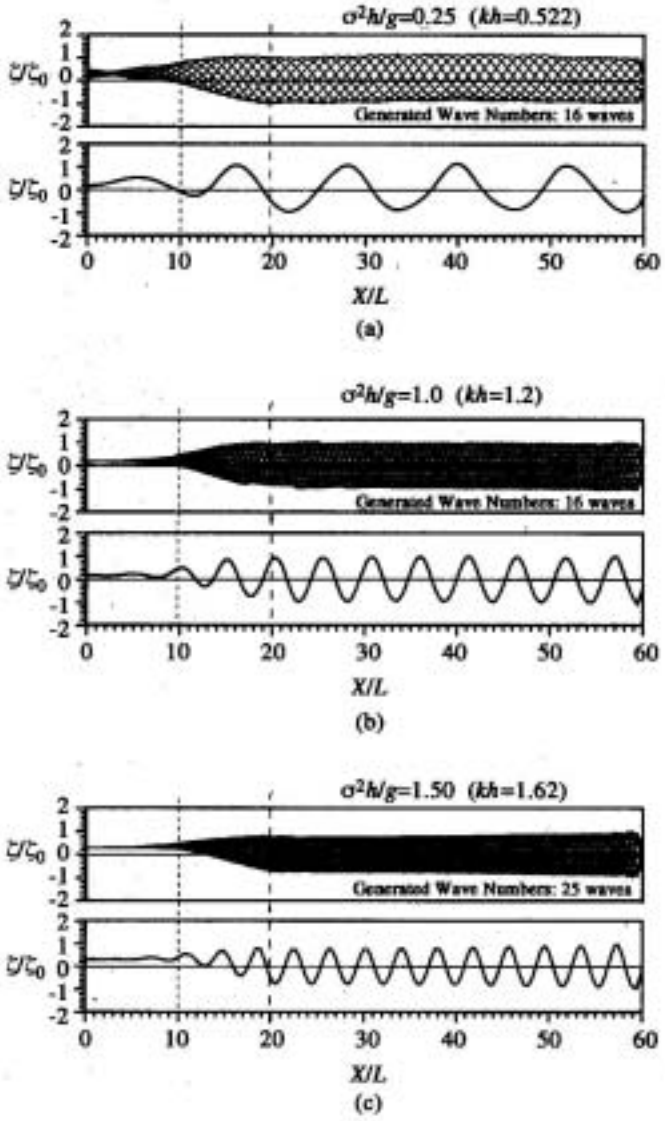

Fig. 7 Time histories of progressing and reflected periodic waves with X=10m, B=10m, σ^2h/g=0.25, 1.0 and 1.50 regarding μ_0=1.0

generated by the moving paddle then propagate toward the sponge zone where they are absorbed almost completely. The efficiency of the combination is also verified by perusing the distribution of wave profiles of other cases with σ^2h/g=0.25, 1.0 and 1.5 as shown in Fig. 7, where the number of generated waves are listed on the figures.

IV. CONCLUSION

In this paper, we present our numerical results of wave generation and the use of absorbing boundary. The results demonstrated the effectiveness of the absorbing boundary in wave damping.

The attenuation rate increases not only with increasing value of the absorbing coefficient, μ_0, but also with the length of the sponge zone, and it is found that better absorption efficiency can be achieved when in the sponge zone a longer X is used instead of B. Nevertheless, when either is used alone, neither of these two factors, i.e., the absorbing coefficient, μ_0, or the length of sponge zone, $X+B$, is sufficient in damping wave energies effectively. Maximum absorption of incident wave energy can only be achieved through an optimum combination of the values of the absorption coefficient μ_0, and the two lengths in the sponge zone, X and B.

Based upon the present results, it is concluded that:

1. For the case of propagation and dissipation of solitary waves, since there's only one wave crest, the attenuation rates can be calculated either by theoretical formula or conservation of mass by comparing the incident and reflected wave height. The optimum combination would be μ_0=0.5, X=15 m and B=10 m, the attenuation rate of the wave energy for this combination approaches 100%. This indicates that wave energy is almost completely dissipated.
2. For cases of fully nonlinear periodical waves, it is difficult to distinguish the reflected waves from the incident waves, the reflection coefficient is not yet clear, therefore we suggest a favorable combination instead, which would be X=10 m and B=10 m, with μ_0=1.0.
3. The numerical scheme will also be extended for the study of irregular waves in our further study.

ACKNOWLEDGEMENT

The authors wish to express their gratitude for the financial aids of the National Science Council, Republic of China, Project No. NSC-89-2611-E-019-027

NOMENCLATURE

B	length of smoothly varied μ area
C	wave celerity
D	Lagrange Differentiation
E	total energy
E_R	total energy of reflected wave
E_I	total energy of incident wave
g	gravitational acceleration
h	water depth
I	unit matrix
k	wave number
K_L	attenuation rate
l	length of sponge zone
n	normal derivative
P	pressure term
s	tangential derivative
T	wave period
t	time
t_c	specific time
U	velocity of wave paddle
X	length of constant μ area

Γ boundary
Δs spatial discretization
Δt time discretization
Φ velocity potential
α exponent value
ζ surface elevation
ζ_0 incident wave height
σ angular frequency
ρ fluid density
μ_0 non-dimensional absorption coefficient
μ absorption term
χ shape function

REFERENCES

1. Brorsen, M., and Larsen, J., 1987, "Source Generation of Nonlinear Gravity Waves with the Boundary Integral Equation Method," *Coastal Engineering*, 11, pp. 93-113.
2. Cao, Y., Beck, R. F., and Schultz, W. W., 1993, "An Absorbing Beach for Numerical Simulations of Nonlinear Waves in a Wave Tank," *Proceedings, 8th Inernational Workshop Water Waves and Floating Bodies*, St. John's: Newfoundland, pp. 17-20.
3. Chou, C. R., 1976, "Investigations of Wave Deformation with the Influence of Coastal Structures," Ph.D. thesis, Kyushu University, Kyushu.
4. Chou, C. R., and Shih, R. S., 1996, "Generation and Deformation of Solitary Waves," *China Ocean Engineering*, Vol. 10, No. 4, pp. 419-432.
5. Dalrymple, R. A., Martin, P. A., and Li, L., 2000, "Waves in Rectangular Inlet with Reflecting or Absorbing Walls," *Journal of Waterway, Port, Coastal and Ocean Engineering*, Vol. 126, No. 6, pp. 288-296.
6. Grilli, S. T., and Subramanya, R., 1995, Recent Advances in the BEM Modeling of Nonlinear Water Waves (Chapter 4). *Topics in BE Applications in Fluid Mechanics*, ed. H. Power, Wessex Institute of Technology: Southampton, pp. 91-122.
7. Grilli, S. T., Svendsen, I. A., and Subramaya, R., 1997, "Breaking Criterion and Characteristics for Solitary Waves on Slopes," *Journal of Waterway, Port, Coastal and Ocean Engineering*, Vol. 123, No. 3, pp. 112-120.
8. Ijima, T., Eguchi, Y., and Kobayashi, A., 1971, "Permeable Breakwater and Seawall," *Proceeding, 18th Japanese Conference on Coastal Engineering*, J.S.C.E., pp. 121-130.
9. Larsen, J., and Dancy, H., 1987, "Open Boundaries in Short Wave Simulations-A New Approach," Coastal Engineering, 7, pp. 285-297.
10. Le Méhauté, B., 1972, "Progressive Wave Absorber," *Journal of Hydraulic Research*, Vol. 10, No. 2, pp. 153-169.
11. Ohyama, T., and Nadaoka, K., 1991, "Development of a Numerical Wave Tank in Nonlinear and Irregular Wave Field with Non-reflecting Boundaries," *Civil Engineering Research*, J.S.C.E., Vol.429(II-15), pp. 77-86.

Manuscript Received: Jan. 17, 2001
Revision Received: July 28, 2001
and Accepted: Aug. 17, 2001

數值造波水槽消能透水層最佳配置之研究

周宗仁　尹彰

國立臺灣海洋大學河海工程學系

石瑞祥

東南技術學院土木工程系

摘　要

本研究以邊界元素法所建立之消波式二維數值造波水槽探討水槽末端假想消能透水層之配置對孤立波與有限振幅週期波之消能效果，考量解析領域速度勢之連續性問題，將此消波區同時分割爲消能係數μ值漸變段及定值段，根據孤立波之消能係數及週期波受反射波影響後之水面波形變化，探討此漸變段長度B、定值段長度X與消能係數μ_0在不同組合下對波浪消波之最佳效果，以探討其最佳之配置方式。經解析後發現對孤立波與週期波分別在μ_0=0.5、X=15 m、B=10 m與μ_0=1.0、X=10 m及B=10 m時有極佳之結果。

關鍵詞：邊界元素，消波邊界，消能透水層，衰減率。